Article:

Tran, CQ, Keyvan-Ekbatani, M, Ngoduy, D et al. (1 more author) (2021) Stochasticity and environmental cost inclusion for electric vehicles fast-charging facility deployment. Transportation Research Part E: Logistics and Transportation Review, 154. 102460. ISSN 1366-5545

https://doi.org/10.1016/j.tre.2021.102460

Stochasticity and environmental cost inclusion for electric vehicles fast-charging facility deployment

Cong Quoc Tran[a,*], Mehdi Keyvan-Ekbatani[a], Dong Ngoduy[b], David Watling[c]

[a] *Complex Transport Systems Laboratory, Civil and Natural Resources Engineering, University of Canterbury, New Zealand*

[b] *Institute of Transport Studies, Monash University, Australia*

[c] *Institute for Transport Studies, University of Leeds, UK*

Declaration of Interest

No potential conflict of interest was reported by the authors.

Corresponding author

Email address: cong.tran@pg.canterbury.ac.nz (Cong Quoc Tran)

Full postal address: 1/313 Waimairi, Ilam, Christchurch, 8041, New Zealand

Stochasticity and environmental cost inclusion for electric vehicles fast-charging facility deployment

Abstract

This study aims to seek the optimal deployment of fast-charging stations concerning the traffic flow equilibrium and various realistic considerations to promote Electric Vehicles (EVs) widespread adoption. A bi-level optimization framework has been developed in which the upper level aims to minimize the total system cost (i.e., capital cost, travel cost, and environmental cost). Meanwhile, the lower level captures travellers' routing behaviours with stochastic demands and driving range limitation. A meta-heuristic approach has been proposed, combining the Cross-Entropy Method and the Method of Successive Average to solve the problem. Finally, numerical studies are conducted to demonstrate the proposed framework's performance and provide insights into the impact of uncertain driving range and charging congestion on the planning decision and the system performance. Generally, both on-route congestion and charging congestion tend to be more serious when there are more EVs in the network; however, the system performance can be improved by increasing EVs' driving range limitation and providing appropriate charging infrastructure.

Keywords: Electric Vehicles, Fast-charging Stations, Bi-level Optimization, Stochastic Driving Range, Charging Congestion, Queuing Theory

1. Introduction

Although the transportation sector has been known as the vital element for socio-economic development, it is one of the main contributors to environmental issues and raises big concern about energy security. This sector accounts for a third of total global greenhouse gas emissions, and it is known to be responsible for significant pollutants that cause serious health problem (Ozbay et al., 2001). Besides adverse effects on the environment, on-route vehicles raise a great concern on energy security. In the US, transportation is responsible for 29% of the total energy consumption, with 92% related to fossil fuel (Ngo et al., 2020). Therefore, people are starting to shift in favour of Electric Vehicles (EVs) to mitigate petroleum dependence and air pollution, marking a new transportation sector era. Billions of dollars in subsidies for charging infrastructure have been provided by governments and automakers worldwide to prepare for the upcoming electrification revolution of transportation (IEA, 2019). The widespread adoption of EVs gives a strong motivation to research problems that study the optimal deployment charging infrastructure, which is the topic of this study.

According to EV travellers' needs, two basic charging facilities are currently deployed: low-power (level 1 and level 2 modes) and fast charging (level 3 mode). This paper focuses on the fast charging infrastructure due to its significant role in alleviating travellers' range anxiety (Wu and Sioshansi, 2017; Guo et al., 2018). Although EVs' driving range has been improved recently, this potential range can be significantly reduced depending on ambient temperatures, driver behaviour, and battery degradation over its expected lifetime (Varga et al., 2019).

Besides, as technology increases, it will be rolled out across heavier vehicles, potentially travelling more considerable distances, making the issue of range pertinent. Indeed, already there are developments in Battery Electric Trucks (BETs) and their potential use in long-haul logistics across Europe. For such vehicles, while 'uncontrolled charging' (when the battery is exhausted) may not be so feasible to plan for, 'opportunity charging' (when loading/unloading or during a driver's rest time) will likely be a key element (Earl et al., 2018), which poses a significant challenge for infrastructure design, not the least of which because of the demands on the electricity grid of the kinds of battery that would be needed.

Another motivation for the need for fast charging location problem with multiple recharges is the comprehensive forecast that personal vehicle ownership will rapidly decrease in the future, and already EVs are a central part of many car-sharing businesses. In this case, an EV can be in almost continuous use; then there will be a need for 'smart charging' approaches to utilise times when the vehicle is idle, and parking which will depend on the availability of such charging infrastructure (Huber et al., 2020).

The charging infrastructure deployment process can be stated as a chicken-and-egg dilemma. Although investment decisions of where to deploy facilities are costly and affect a long-time horizon, the charging stations need to be provided before observing the actual demand. It emphasises the stochastic nature of the charging facilities planning problem. Therefore, we put our effort to capture three primary sources of uncertainty in the present paper: travellers' demands, EVs' driving ranges and route choice behaviours.

Finally, the electrification of transportation and infrastructure deployment also result in changes in traffic flow. Although more EVs can bring a cleaner and more energy-efficient transportation system, it sometimes may cause more congestion over the network (i.e., en-route and charging congestion) (Tran et al., 2021). Therefore, it is crucial to develop a systematic framework for deploying charging infrastructure to minimise the capital cost and reduce the congestion and environmental cost with consideration of stochastic driving range, charging congestion, and the mutual interaction between charging locations and traffic flow pattern.

1.1. Background works

The EVs-charging facility location problem can be generally categorised into node-based, flow-based and equilibrium-based approaches depending on the charging demand pattern and route choice behaviours (Shen et al., 2019). The original node-based model was proposed based on the concept of covering demand nodes (Church and Meadows, 1979). With the assumption of having demand at individual nodes, this approach maximises demand coverage (maximal covering location models) or minimises the number of required facilities (set covering location models). In the presence of EVs, node-based models are suitable for locating on-site low-power facilities where EVs' users can park their cars for several hours for fully recharge (Nozick, 2001; He et al., 2016).

On the other hand, the flow-based approach considers demands in the form of traffic flow, which makes these models more preferable for on-route fast-charging facilities due to their ability to capture users' behaviour. However, the first flow-based models are unable to capture the limited driving range of EVs. It leads to the assumption that travellers always choose the flow-independent shortest path, and all of the path flow can be captured as long as there is a charging station on this path Hodgson (1990). Based on the first flow-capturing location model, the flow-based approach has attracted more extensive investigation and has been extended to allow multiple recharging or necessary deviations from the shortest path (Kuby and Lim, 2005; Upchurch et al., 2009; Wang and Lin, 2009; Kim and Kuby, 2012; Li and Huang, 2014).

In addition to node-based and flow-based models, the equilibrium-based approach is adopted to avoid network performance deterioration because of the mutual interaction of re-routing behaviours and the charging locations decision. The problem can be formulated as a bi-level program in which the deterministic or stochastic user equilibrium (DUE or SUE) is included at the lower level. The traffic assignment problem with EVs' presence needs to consider the charging nature and the limited driving ranges. He et al. (2014) formulated three mathematical models considering flow dependency of energy consumption and recharging time to describe network equilibrium flow.

Most of the studies adopt the DUE or logit-based SUE to model the drivers' behaviour in the literature. Although the probit-based SUE can better capture the realistic route choice decision, it is less attractive to the scholars because of lacking a closed-form formula for calculating route choice probabilities and computational complexity. According to the flow-based and equilibrium-based approach, a summary of some recent studies is presented in Table 1.

Table 1: Some recent studies on EVs charging facility location problem

Approach	**Study**	**Objective**	**Considerations**	**Model**	**Solution**	**Evaluation**
Flow-based	Hosseini et al. (2017)	Maximize the total covered flow	– Shortest path with deviation – Capacitated facilities	MILP	Heuristic	Numerical tests
	Wu and Sioshansi (2017)	Maximize expected captured flows	– Shortest path with deviation – Uncertain EVs flow	Two-stage stochastic integer linear program	Sample-average approximation method	Case study
	Xie et al. (2018)	Minimize – investment cost (fixed and variable cost), and – cost associated with unsatisfied BEVs trips	– Shortest path with deviation – Chance constraint on level of service – Charging station capacity	Multistage chance-constrained stochastic model	Genetic algorithm	Case study
	Xu et al. (2020)	Minimize the accumulated range anxiety of concerned travelers	– Shortest path with deviation	MINP	Outer-approximation method	Numerical tests; Case study
	Xu and Meng (2020)	Maximizing the covered path flows	– Shortest path with deviation – Nonlinear elastic demand	MIP	Tailored branch-and-price method	Numerical tests; Case study
Equilibrium-based	Jing et al. (2017)	Maximize coverage of EVs flows	– Mixed vehicle classes – Route choice behaviours (logit-based SUE) – Multiple stops for recharging	Bi-level	Equilibrium-based heuristic	Numerical tests

continued ...

. . . continued

Approach	Study	Objective	Considerations	Model	Solution	Evaluation
	Zheng et al. (2017)	Minimize – travel time, and – energy consumption	– Route choice behaviours (DUE)	Bi-level; Single-level reformulation	CPLEX	Numerical tests
	Guo et al. (2018)	Minimize – total construction cost, and – EVs path deviation cost	– Shortest path with deviation – Satisfy a planned proportion of EV users	Bi-level	Adaptive large-neighborhood search	Case study
	Zhang et al. (2018)	Minimize – system travel cost, and – greenhouse emissions	– Multitype recharge facility – Mixed vehicle classes – Route choice behaviours (DUE) – Multiple stops for recharging	Bi-level	Genetic algorithm	Numerical tests
	He et al. (2018)	Maximize captured flows	– Route choice behaviours (DUE)	Bi-level; single-level reformulation	CPLEX	Numerical tests
	Huang and Kockelman (2020)	Maximize the profit of station placement	– Route choice behaviours (DUE with elastic demand) – Station congestion	Bi-level	Genetic algorithm	Case study
	Ngo et al. (2020)	Minimize – total system travel time, or – total system net energy consumption	– Wireless charging infrastructure – Route choice behaviours (DUE) – Constraints on completion reassurance and equity in resource distribution	Bi-level	Constrained local metric stochastic response surface algorithm	Numerical tests; Case study

continued . . .

. . . continued

Approach	Study	Objective	Considerations	Model	Solution	Evaluation
	Tran et al. (2021)	Minimize – total investment cost, and – system travel cost	– Mixed vehicle classes – Route choice behaviours (DUE) – Multiple stops for recharging – Changes of EVs penetration	Bi-level	Cross-entroy method-based algorithm	Numerical tests

In our study, we define the driving range limitation of an EV as the maximum distance that the vehicle can travel with a full battery. To incorporate EVs driving range limitation when modelling the relationship between charging locations and the feasibility of travelling paths, one can use the energy conservation logic to identify the state of charging (SOC) of the vehicle at each specific location (node) given a fixed driving range limitation or the capacity of EVs' battery. SOC can be modelled as a function of travel distance or travel time. In the case SOC is modelled as a function of travel distance, the max SOC can be defined as the max distance an EV can travel with a full battery. Then, a path is defined to be feasible if and only if the SOC is non-negative at all nodes along the path.

With the detailed consideration of SOC changes, one also can investigate the concept of range anxiety which can be accumulated and built up over a journey by accumulating all the anxieties travellers felt during their trip, as the battery charge changed and as they went through various charging stations (Xu et al., 2020). In the study of Xu et al. (2020), which is dealing with the accumulated range anxiety by the time a driver has arrived at their destination, the range anxiety must be tracked as it varies during a journey (Figure 2) since the authors aim to minimize an objective function which includes the accumulated range anxiety. However, in our paper, we only consider physical characteristics of driving range instead of tracking how range anxiety varies within a trip.

Although there are a substantial number of EVs-charging facility location models in the literature in which EVs' driving range limitation is assumed to be fixed and known in advance (Jiang et al., 2014; Jing et al., 2017; Xie et al., 2018; He et al., 2018; Guo et al., 2018), there are several reasons why the range may vary in some unpredictable way, suggesting that it may be better represented as a stochastic variable. Influential features include battery condition, initial charge, traffic condition, driving behaviour, or weather (Lee et al., 2014; Dong and Lin, 2014; de Vries and Duijzer, 2017). As one of the first attempts to incorporate stochastic driving range, Lee et al. (2014) assume a randomly distributed remaining fuel range at the origin node of a trip, where the driving range is sufficient to cover all O-D pairs such that travellers need to recharge at most once during their trip. Another approach is to include the driving range explicitly as a parameter and maximize the expected number of drivers who can complete the trip without running out of battery using a chance constraint on the driving range (de Vries and Duijzer, 2017; Lee and Han, 2017; Boujelben and Gicquel, 2019).

Besides the driving range limitation, the charging demand is also highly stochastic. Considering the uncertainty in EVs' flows, many studies adopt the two-stage optimization approach to deal with the imperfect demand information. Hosseini and MirHassani (2015) introduced a two-stage model to locate permanent stations and then locate portable stations at the second stage. Similarly, Wu and Sioshansi (2017) proposed a two-stage stochastic flow-capturing location model to maximize the expected capture flows in which the first stage determines a fixed number of charging stations and the second stage determines which EVs can be captured by the built charging stations. Yang et al. (2017) presented a swapping/charging station network problem using fuzzy optimization approach considering fuzzy customer perception related to range anxiety and loss anxiety. Furthermore, considering the charging station capacity and the increasing EVs' penetration, it is more practical to account for the charging congestion and number of chargers located at each station. By adopting queuing theory, Xiao et al. (2020) used the point-based approach to determine the optimal locations and capacities of charging stations considering charging queue behaviour with finite queue length. On the other hand, Yıldız et al. (2019) adopted the flow-based approach and scenario-based approach to address the problem considering stochastic recharging demands, capacity limitations for the charging stations and travellers' route deviation tolerances.

Xie et al. (2018) introduced a multistage chance-constrained stochastic model to support planning and operational decisions. In planning decisions, the model determines where and how many chargers need to be deployed to satisfy the growing EV travel demand with deterministic driving range. On the other hand, operational decisions on path selection and charging scheme are made along with each feasible O-D pair. Besides, a chance-constrained is formulated to identify the required number of chargers to meet a charging capacity level. Nevertheless, incorporating the uncertain driving range, travel demand and charging congestion into the charging facility location problem with equilibrium-based approach are still potential research gaps in the literature.

1.2. Objectives and contributions

Having the aforementioned motivation and research gaps in mind, the overall objective of the present paper is to optimally deploy fast-charging stations in the manner of minimizing the expected system cost. Furthermore, the drivers' route choice behaviour under stochastic demand and driving range limitation is recognized and incorporated into the model. This study contributes to the literature in the following aspects:

1. A systematic framework is proposed to solve the charging facility location problem, which simultaneously takes into account the investment cost, congestion (i.e., en-route congestion and charging congestion) and the environmental cost. To the best of our knowledge, this paper is the first one that jointly considers:
   - stochastic travelling and charging demands
   - stochastic driving range limitation of EVs
   - charging congestion at charging stations
   - travellers route choice behaviors (probit-based SUE)
2. A meta-heuristic is proposed to mimic the highly stochastic nature of the decision-making process. Numerical tests have shown that the proposed approach can efficiently find a good solution by which the planners can capture more realistic considerations.

The remainder of the paper is organized as follows. The bi-level optimization framework for seeking the optimal solution of charging stations and the number of chargers is described clearly in Section 2. In Section 3, a meta-heuristic is developed to solve the problem. Numerical experiments are conducted in Section 4. Finally, Section 5 concludes the paper and suggests potential future research directions.

1.3. Notations and assumptions

The used notations are described as in Table 2. Sets or random variables are expressed in capital letters and vectors or matrices are expressed in bold font.

Table 2: Table of notation

Symbol	Definition
	Sets and parameters
K	Set of nodes, $k \in K$
A	Set of links, $a \in A$
W	Set of all O-D pairs, $w \in W$
N	Set of vehicle classes, $n \in N$
P^w	Set of all path p between O-D pairs $w \in W$, $p \in P^w$
t_a^0	Free-flow travel time of link a
c_a	Capacity of link a
l_a	Length of link a
l_p^w	Length of path p between O-D pair w
$l_{s,p}^w$	Length of sub-path s on path p between O-D pair w
m	Maximum number of chargers of each charging station
c_k	The fixed cost of opening a charging station at node k
h_k	The unit cost of installing one charger at node k
μ_k	The charging (service) time at each charging node k
v_1	The monetary value of travel time
v_2	Unit cost of CO per ton
$\delta_{k,p}^w$	Node-path incidence, which equals 1 if node k is on path p between pair w and 0 otherwise
$\delta_{a,p}^w$	Link-path incidence, which equals 1 if link a is on path p between pair w and 0 otherwise
D^n	Random driving range limitation of vehicle class n
$Q^{w,n}$	Random travel demand of vehicle class n between O-D pair w
$q^{w,n}$	Mean of travel demand of vehicle class n between O-D pair w
	Decision variables
x_k	Whether a charging station is located at location k or not
$\mathbf{x}$	Vector of all charging locations
u_k	Number of chargers placed at location k
$\mathbf{u}$	Vector of all number of chargers
$y_{p,n}^w$	Whether path p between pair w is feasible for vehicle class n or not
$\mathbf{y}$	Vector of all feasible paths
Q_a	Random variable of aggregate traffic flow on link a
q_a	Mean of aggregate traffic flow on link a
q_a^n	Mean of traffic flow of vehicle class n on link a
T_a	Random variable of travel time on link a
t_a	Mean of travel time on link a
$F_p^{w,n}$	Random variable of traffic flow of vehicle class n on path p between O-D pair w
$f_p^{w,n}$	Mean traffic flow of vehicle class n on path p between O-D pair w
$\mathbf{f}$	Vector of all mean path flows
T_p^w	Random variable of travel times on path p between O-D pair w
t_p^w	Mean travel time on path p between O-D pair w
$\mathbf{t}^w$	Column vector of all perceived path travel times between O-D pair w, $\mathbf{t}^w = (t_p^w)^T$
λ_k	Mean arrival rates of EVs at charging station k
w_k	The expected waiting time at charging station k

continued ...

. . . continued

Symbol	Definition
e_a^g	The average amount of traffic emissions cause by GVs on link a
$\mathbb{G}_{s,p}^{w,n}$	Probability that driving range D^n is smaller than the length of sub-path s of path p
$\mathbb{P}_p^{w,n}$	Probability that vehicle class n choose path p between O-D pair w

To simplify the problem, the following reasonable assumptions are made in the present study.

I. In this study, we focus on physical characteristics of driving range limitation instead of tracking how range anxiety varies within a trip. Within the scope of the study, we assume the maximum driving range between full charge and no-charge of an EV is a stochastic parameter. For a given realization of the random conditions ω, the driving range of vehicle class n, $D^n(\omega)$ is the same for each sub-path and randomly distributed with cumulative density function $G^n : \mathfrak{R}_+^n \to [0, 1]$. Consequently, the driver might not be willing to take a trip if the probability of running out of fuel during this trip is above a maximum acceptable risk threshold $\alpha \in [0, 1]$.

II. To capture the stochastic travel demand in route choice decision, we assume that the travel demands of vehicle class n between O-D pairs w follow independent stationary Poisson distribution with constant mean (and variance) $q^{w,n} > 0$. Besides, travellers have perceptual differences in their evaluation of a given travel time and make the decision independently between alternative paths $p \in P^w$ with probabilities $\mathbb{P}_p^{w,n}$ for each $n \in N$ and $w \in W$.

III. In reality, the waiting time at charging stations contributes an insignificant amount to the path travel time; therefore, it is reasonable to assume that travellers only consider the path feasibility and the link travel times in their route choice decision process. This argument can be proved by comparing total waiting time and travel time through numerical tests (Figures 7a - 7b) and Appendix C.

IV. In order to examine the charging congestion at charging stations, we consider the arrival rate at each charging station as a function of EVs path flow, $\lambda = \lambda(\mathbf{f})$. Besides, each charger is assumed to have an independently and identically distributed exponential charging time, μ. Due to the condition for stationary distribution, the arrival rate is assumed to be smaller than the service rate.

2. Bi-level planning framework

In this section, we put our effort to propose a planning framework to optimally identify the locations and number of chargers at each fast-charging station to minimize the expected system cost. The expected system cost consists of the capital cost of the charging infrastructure, the expected monetary value of total travel time and the environmental cost.

The capital cost incurred by installing charging stations and placing the chargers at each station. The station installation costs may include site acquisition, utility provision, permitting, project management, etc., which can be estimated based on the average cost in a particular study area while the charger unit cost can be found varied due to the providers (Ghamami, 2019). In this study, we constrain the maximum number of chargers deployed at each charging station to represent the budget and capacity limitation. One can easily modify this constraint subject to the practical purpose of the study.

The second term of the objective function is the expected monetary value of total travel time. The total travel time includes the expected en-route travel time and expected charging time at charging stations which are resulted from the route choice behaviour of travellers. In this study, a multi-class probit-based SUE model with Poisson demand (probit-based SUE-P) is used to model the traffic flow equilibrium. In comparison with GVs, EVs' users choose the route to minimize their perceived travel times and have to consider the feasibility of the selected route. Besides, to capture the problem's stochastic nature, we imply a chance constraint on the driving range and adopt the queuing theory to project the charging congestion. It is worth to note that in this study, EVs' drivers are allowed to have multiple en-route recharging with the stochastic charging demand.

The final term of the objective function is the environmental cost. On-road vehicles have been known as a significant contribution to air pollution, including carbon monoxide (CO), volatile organic compounds (VOC), nitrogen oxides (NO_x) and particulate matter (PM). In fact, on-road vehicles are responsible for most of CO emissions in the air (Yin et al., 2014). In this paper, therefore, we consider CO as an indicator of the level of air pollution generated by GVs while EVs can be seen as zero-emission vehicles. The total amount of traffic emissions can be calculated by the product of the average amount of traffic emissions and the GVs traffic flow on the network and converted into the monetary value by CO unit cost.

To sum up, the problem can be generally formulated as a bi-level framework as in Figure 1.

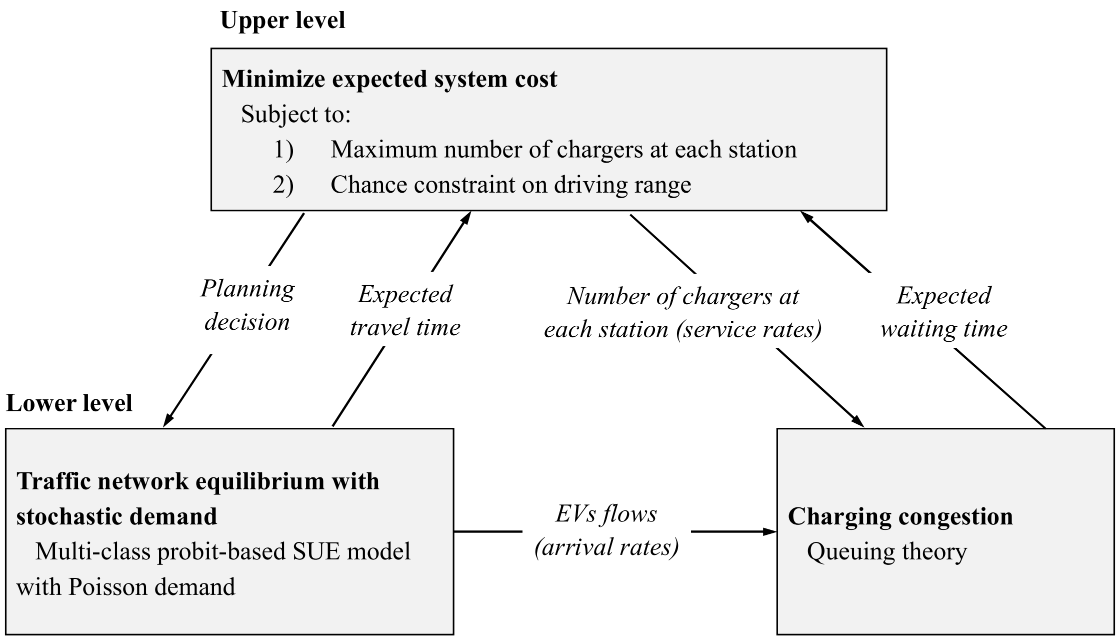

Figure 1: The bi-level optimization framework

The feasibility of paths for EVs can be identified using the concept of sub-path (Xie and Jiang, 2016; Tran et al., 2021). For a given set of charging stations, the sub-paths of a path include the route from the origin to the first charging station, from a charging station to the following charging station and from the last charging station to the destination (Figure 2). With the fixed and pre-determined driving range limitation, a path is feasible only if all sub-paths are less than the EVs' driving range. To capture the driving range limitation, one can put the constraints ensuring that a path is feasible for a vehicle if only this vehicle can traverse all the sub-paths without running out of battery as in constraints (1) and (2).

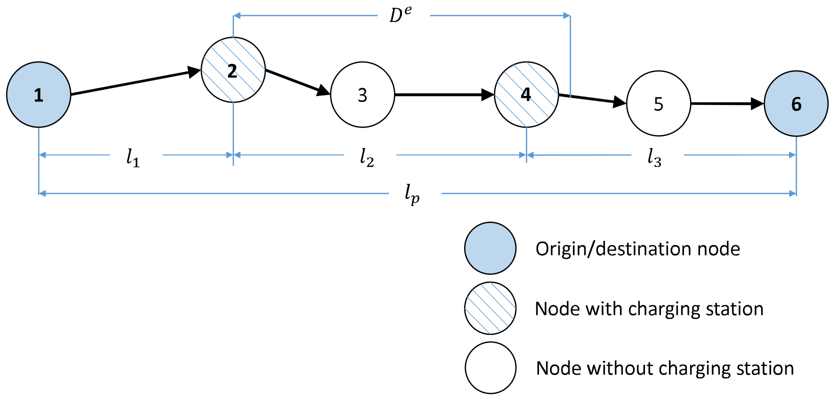

Figure 2: Illustration of sub-paths (Tran et al., 2021)

$$\left[D^n - \max\left(l^w_{s,p}\right)\right] y^{w,n}_p \geq 0 \qquad \forall w \in W, n \in N, p \in P^w \tag{1}$$

$$y^{w,n}_p > \frac{D^n - \max\left(l^w_{s,p}\right)}{D^n} \qquad \forall w \in W, n \in N, p \in P^w \tag{2}$$

To incorporate the stochastic driving range limitation, we consider the driving range (maximum distance an EV can travel between full charge and no-charge) as a stochastic parameter. Figure 3 has conceptually presented our idea of tracking a journey for different vehicles (with the different initial charge, charging capability, weather condition, etc.) to show the variance on driving range limitation we are trying to capture.

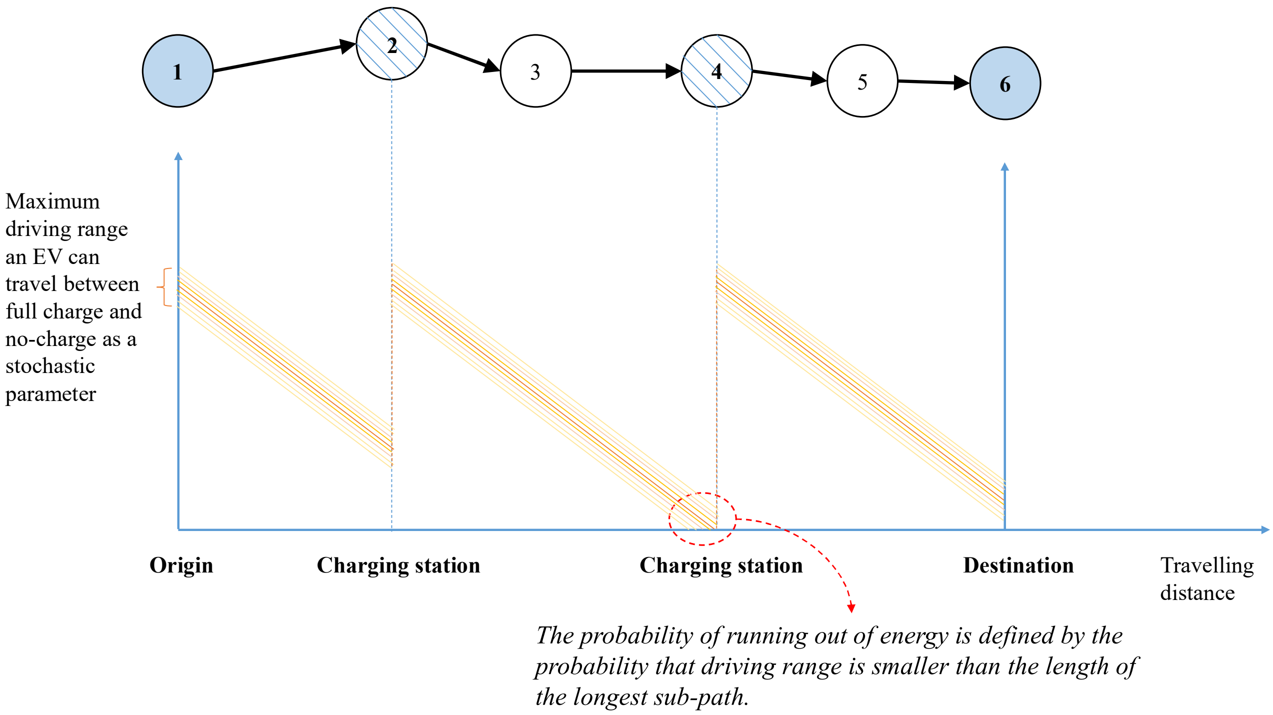

Figure 3: The stochastic driving range and probability of running out of energy over path

Under assumption (I), the probability of running out of energy equals the smallest probability that the driving range exceeds the length of a sub-path among all sub-paths of this path (de Vries and Duijzer, 2017). In other words, it is the probability that driving range is smaller than the length of longest sub-path which is illustrated in Figure 3. Let $\mathbb{G}_{s,p}^{w,n}$ denote the probability that driving range D^n is smaller than the length of sub-path s of path p.

$$\mathbb{G}_{s,p}^{w,n} = \mathbb{P}\left(D^n \leq l_{s,p}^w\right) = G^n(l_{s,p}^w) \tag{3}$$

EV drivers are assumed to be willing to take a trip if the probability of running out of fuel during this trip is under a maximum acceptable risk threshold, α. In the case of stochastic driving range, constraints (1) and (2) then be replaced by the chance constraint (4).

$$\mathbb{G}_{s,p}^{w,n} \leq \alpha + \left(1 - y_p^{w,n}\right) \qquad \forall w \in W, n \in N, p \in P^w \tag{4}$$

Due to the linearity, constraint (4) can be relaxed into an equivalent deterministic expression using the probability density function to calculate the probability $\mathbb{G}_{s,p}^{w,n}$.

2.1. The upper-level planning

At the upper level, the planner aims to minimize the expected system cost, which includes the charging infrastructure investment cost, the expected travel cost and the environmental cost. The objective function is presented as a performance index (PI) function, which can be calculated by the vector of locating solutions $\mathbf{X}$ and the corresponding vector of equilibrium link flows $\mathbf{f}$, denoted as PI($\mathbf{X}, \mathbf{f}$).

$$\min_{(\mathbf{X},\, \mathbf{f})} \quad \mathrm{PI}(\mathbf{X}, \mathbf{f}) = \sum_{k \in K} (c_k x_k + h_k u_k) + v_1 \left[\sum_{w \in W} \sum_{p \in P^w} \sum_{n \in N} \mathbb{E}(T_p^w)\mathbb{E}(F_p^{w,n}) + \sum_{k \in K} W_k \lambda_k\right] + v_2 \sum_{a \in A} \mathbb{E}(Q_a^g) e_a^g \tag{5}$$

The vector $\mathbf{X}$ includes the vector of charging locations $\mathbf{x}$, the vector of number of chargers $\mathbf{u}$, and a corresponding vector of feasible paths $\mathbf{y}$. Changing the charging locations and number of chargers at each station may cause the changing of feasible paths, which leads to re-routing of traffic, hence $\mathbf{f} = \mathbf{f(X)}$.

The feasible space of locating solutions, Ω, then can be explicitly defined as follows.

$$u_k \leq m x_k \qquad \forall k \in K \tag{6}$$

$$\mathbb{G}_{s,p}^{w,n} \leq \alpha + \left(1 - y_p^{w,n}\right) \qquad \forall w \in W, n \in N, p \in P^w \tag{7}$$

$$x_k = \{0, 1\} \qquad \forall k \in K \tag{8}$$

$$y_p^{w,n} = \{0, 1\} \qquad \forall w \in W, n \in N, p \in P^w \tag{9}$$

$$u_k \geq 0 \qquad \forall k \in K \tag{10}$$

Constraint (6) entails the maximum number of charging stations to be located (according to a given budget). Constraint (7) ensures that a path is feasible for a vehicle if only the probability that a trip along path p can be made without running out of fuel at most α.

The expected time at charging station k (W_k) is a function of the number of chargers (u_k), the arrival rate of EVs (λ_k) and the service rate of charging station (μ_k), $W_k = W_k(u_k, \lambda_k, \mu_k)$. The arrival rates at charging stations can be inferred from the corresponding SUE flows. The resulting expected waiting time at charging stations, $W(u, \lambda, \mu)$ then can be obtained in a recursive manner as following (Berman and Drezner, 2007; Jung et al., 2014).

$$a_1 = 1; a_i = 1 + \frac{\mu}{\lambda}(i-1)a_{i-1} \tag{11}$$

$$W(u, \lambda, \mu) = \frac{\lambda}{(u\mu - \lambda)^2 \left[a_u + \frac{\lambda}{(u\mu-\lambda)}\right]} + \frac{1}{\mu} \tag{12}$$

Among the significant pollutants emitted from gasoline vehicles, we use carbon monoxide (CO) to indicate the level of air pollution. By adopting the study of Penic and Upchurch (1992), the average amount of CO emission on a link can be estimated as a function of link travel time as in (13).

$$e_a^g = \rho_1 \hat{t}_a exp\left(\rho_2 \frac{l_a}{\hat{t}_a}\right) \tag{13}$$

where ρ_1 and ρ_2 are constants with values of 11.063927 and 0.008493, respectively (Yin et al., 2014).

2.2. The lower-level traffic assignment problem

At lower level, the equilibrium traffic flow is determined by solving a mixed-flow SUE traffic assignment with Poisson O-D demand and multinomial conditional route choice. In our study, the equilibrium flows $\mathbf{f}$ is corresponded to each locating solution $\mathbf{X}$, $\mathbf{f} = \mathbf{f(X)}$. In the light of assumption (II), the travel demand between O-D pair w are assumed to be Poisson, $Q^w \sim Poisson(q^w)$. Consequently, the resulting path flows of each vehicle class n between O-D pair w follow independent Poisson distribution, $F_p^{w,n} \sim Poisson(f_p^{w,n})$ (Clark and Watling, 2005; Nakayama and Watling, 2014) with the mean path flow which are the solution to the following equivalent fixed-point problem.

$$f_p^{w,n} = q^{w,n}\mathbb{P}_p^{w,n}(\mathbf{t}^w(f)) \qquad \forall w \in W, n \in N, p \in P^w \tag{14}$$

$\mathbb{P}_p^{w,n}$ denotes the probability that vehicle class n choose path p between O-D pair w.

$$\mathbb{P}_p^{w,n} = \mathbb{P}\left(t_p^w \leq t_l^w, \forall l \in P^w, l \neq p | y_p^{w,n} = 1\right) \tag{15}$$

Besides, the link flow random variables Q_a are marginally Poisson which are related to the path flow variable via (16) with the mean identified in (17).

$$Q_a = \sum_{w \in W} \sum_{p \in P^w} \sum_{n \in N} \delta_{a,p}^w F_p^{w,n} \qquad \forall a \in A \tag{16}$$

$$q_a = \sum_{w \in W} \sum_{p \in P^w} \sum_{n \in N} \delta_{a,p}^w f_p^{w,n} \qquad \forall a \in A \tag{17}$$

In addition, link travel times T_a are also random variables with the mean that can be determined by a polynomial form as $t_a(q_a) = \sum_{j=0}^{e} b_{ja} q_a^j$. In the present study, we adopt the Bureau of Public Roads (BPR) function as in (18) and use Taylor series approximating to calculate coefficients b_{ja}. Considering the quadratic form of link travel times (e = 2), the modified travel time functions under Poisson demand are presented in (19) (Clark and Watling, 2005). The perceived path travel time are identical for all vehicle classes with the mean defined as in (20).

$$t_a = t_a^0 \left[1 + 0.15\left(\frac{q_a}{C_a}\right)^4\right] \qquad \forall a \in A \tag{18}$$

$$\hat{t}_a = t_a + b_{2a} q_a \qquad \forall a \in A \tag{19}$$

$$t_p^w = \sum_{a \in A} \hat{t}_a \delta_{a,p}^w \qquad \forall p \in P^w \tag{20}$$

The feasible space of path flow solutions, Θ, can be defined by the flow conservation and following constraints. The side-constraints on feasible path flow due to limited feasible paths are shown as constraint (21) in which M is a large positive number. Finally, constraint (22) ensures the positive value of path flows.

$$f_p^{w,n} \leq M y_p^{w,n} \qquad \forall w \in W, n \in N, p \in P^w \tag{21}$$

$$f_p^{w,n} \geq 0 \qquad \forall w \in W, n \in N, p \in P^w \tag{22}$$

2.3. Implicit bi-level programming formulation

The general formula of the bi-level problem can be defined as in (23) with the lower level defined as an equivalent minimization (Sheffi, 1985).

$$\begin{aligned} \min_{(\mathbf{X},\,\mathbf{f})} \quad & \mathrm{PI}(\mathbf{X},\,\mathbf{f}) = \sum_{k\in K}(c_k x_k + h_k u_k) + v_1\left(\sum_{w\in W}\sum_{p\in P^w}\sum_{n\in N} t_p^w f_p^{w,n} + \sum_{k\in K} W_k\lambda_k\right) + v_2 \sum_{a\in A} q_a^g e_a^g \\ \text{s.t.} \quad & \mathbf{X}(\mathbf{x},\,\mathbf{u},\,\mathbf{y}) \in \Omega \\ & \mathbf{f} \in \operatorname{argmin}\left\{Z(\mathbf{f}) = -\sum_{w\in W}\sum_{n\in N} q^{w,n}\mathbb{E}\left[min_{p\in P^w}\{t_p^w\}|\mathbf{t}^w(\mathbf{f})\right] + \sum_{a\in A} q_a t_a(q_a) - \sum_{a\in A}\int_0^{q_a} t_a(q_a)dq : \mathbf{f}\in\Theta\right\} \end{aligned} \tag{23}$$

The proposed bi-level framework is strong NP-hard due to the binary-type decision variables, stochasticity, and intractable structure. Therefore, it is non-viable to find an exact global solution to the problem. Instead, the meta-heuristic approach, such as Genetic Algorithm, Hill Climbing, Simulated Annealing, etc., usually might be applied to obtain a good solution in a reasonable amount of time. The comparison of such different algorithms is beyond the scope of this study. In the present paper, we have adopted a relatively new approach based on the Cross-Entropy Method due to its robustness and insensitivity to the initial solutions. The details of the solution algorithm are presented in the next section.

3. Solution algorithm

The Cross-Entropy Method (CEM) was initially proposed by Rubinstein and Kroese (2004) as an adaptive variance minimization algorithm for estimating rare events probabilities on stochastic networks. Eventually, this method was adopted to effectively solve both static and noisy combinatorial optimization problems, including network design problems in the transportation field (Ngoduy and Maher, 2012; Maher et al., 2013; Zhong et al., 2016; Abudayyeh et al., 2018, 2021). In general, the CEM consists of two steps:

1. Generating the sample of candidate solutions using a given parameterized distribution;
2. Updating the sampling distribution parameters to steer the problem towards the optimal solution over subsequent iterations.

The details of the CEM-based algorithm applied to solve the deterministic fast-charging facility deployment problem as the bi-level program has been proposed in the study of Tran et al. (2021). In the present paper, we extend this approach to consider the environmental cost, stochastic driving range, stochastic charging demand and charging congestion. Furthermore, the changes in EVs market share can also be captured with the continued use of installed charging facilities in later stages. The details of the CEM-based algorithm is presented in Appendix A.

In summary, the CEM-based algorithm implemented for solving the proposed charging facility location problem is shown in Algorithm 1.

Algorithm 1 The CEM-based algorithm

input: network parameters, m, c, h, μ, v_1, v_2
output: $\mathbf{X}$, $\mathbf{f}$

$\gamma \leftarrow \gamma^{(1)}$
$i \leftarrow 1$
while stopping condition is not reached **do**
  $\mathbf{x} \leftarrow \mathrm{S}(N, \gamma^{(i)}, m)$ ▷ randomly sampling location of charging stations and number of chargers
  $\mathbf{y} \leftarrow \mathrm{F}(\mathbf{x}, D^n)$ ▷ identifying corresponding feasible paths using chance constraint
  $\mathbf{f}(\mathbf{X}) \leftarrow$ Probit-based SUE-P($\mathbf{X}$) ▷ the equilibrium flow obtained using Algorithm 2
  $\lambda \leftarrow \lambda(\mathbf{f})$ ▷ calculating arrival rates at charging stations
  $W \leftarrow W(u, \lambda, \mu)$ ▷ estimating waiting time using (11) and (12)
  $e_a^g \leftarrow e_a^g(\hat{t}_a)$ ▷ calculating amount of CO emission on each link via (13)
  $\mathrm{PI} \leftarrow \mathrm{PI}(\mathbf{X}, \mathbf{f}(\mathbf{X}))$
  $N_e \leftarrow$ Select the best 100ρ % of PI values
  $\gamma_{new}^{(i)} \leftarrow$ Update γ using formula (A.3)
  $\gamma^{(i+1)} \leftarrow \alpha\gamma_{new}^{(i)} + (1-\alpha)\gamma^{(i)}$ ▷ parameter vector smoothing
  $i \leftarrow i + 1$

Algorithm 2 The MSA algorithm for multi-class probit-based SUE-P

input: $\mathbf{X}$
output: $\mathbf{f}$

$q_a^n \leftarrow \mathrm{SNL}\big(t_a^0, y^n\big)$ ▷ calculating initial link flow of each vehicle class by performing stochastic network loading based on the feasible path sets
$q_a \leftarrow \sum_n q_a^n$ ▷ identifying aggregate link flow
$i \leftarrow 1$
while stopping condition is not reached **do**
  $\hat{t}_a^{(i)} \leftarrow \hat{t}_a\left(q_a^{(i)}\right)$ ▷ calculating the modified travel time under Poisson demand
  $q'^{n(i)}_a \leftarrow \mathrm{SNL}\left(\hat{t}_a^{(i)}, y^n\right)$ ▷ identifying auxiliary link flow of each vehicle class
  $q_a^{n(i)} \leftarrow q_a^{n(i-1)} + \frac{1}{i}\left(q'^{n(i)}_a - q_a^{n(i-1)}\right)$ ▷ finding the new aggregate link flow
  $q_a^{(i)} \leftarrow \sum_n q_a^{n(i)}$

In this paper, we use the convergence between best PI (upper bound) and worst PI (lower bound) during the last two consecutive iterations as the stopping condition for Algorithm 1 while setting the maximum number of iterations has been reached for Algorithm 2. Otherwise, one can stop the CEM procedure when the distance between two consecutive parameter vectors is sufficiently small.

4. Numerical tests

Two numerical tests have been conducted in this section to illustrate the efficacy of the proposed framework. The model is firstly tested in a medium-sized network (Figure 4) with different scenarios of EVs' driving ranges and charging demand. In the second test, we employ the framework on a large-scale network (Figure 9) and compare the results with those provided by the traditional two-stage optimization approach (Hosseini and MirHassani, 2015; Wu and Sioshansi, 2017) to shed some lights on the solution quality. In this study, the networks are used by both EVs and conventional gasoline vehicles (GVs).

Without loss of generality, we assume the link length is the same as free-flow travel time in the number which is labelled on each link, and the capacity of each link is 1,800 veh/h/lane. In numerical tests, the aggregate travel demands between O-D pairs are assumed to be independent stationary Poisson with the mean and variance of 3,000 veh/h. The aggregate travel demands are chosen for the convenience of analyzing the impact of en-route and charging congestion. Lacking the appropriate data, we assume all paths between the O-D pair are feasible for GVs due to their relatively long driving ranges (Jiang et al., 2014) and the EVs driving ranges follow Gamma distribution due to its flexibility (de Vries and Duijzer, 2017). The maximum acceptable risk threshold in both cases is assumed to be 0.05. Besides, the value of time for all vehicle class is \$20 per hour (Xu et al., 2017), the cost of opening a new charging station and installing a charger are \$250,000 and \$5,000 respectively regardless of its location (EVSE, 2019).

In the CEM-based algorithm, we first choose the typical sample size in the literature $N = 1,000$ and the elite sample proportion $\rho = 1\%$. At each iteration, the parameter vector is updated using the smoothing rate $\alpha = 0.7$. The stopping condition is zero difference between the upper and lower bounds during the last two consecutive iterations. All instances are solved using Python programming language on a computer equipped with Intel(R) Core(TM) i7-7700 CPU @ 3.60GHz and usable RAM of 15.9 GB, running on Windows 10.

4.1. Test-bed network 1: The CEM-based framework

In this subsection, we solve the problem of deploying charging facilities in a medium-sized network consisting of 24 nodes and 38 one-lane directed links. The network is used by mixed EVs and GVs with the aggregate travel demands between O-D pairs as in Figure 4. Link lengths and free-flow travel times are also given in the figure. To gain insights on the impact of EVs driving ranges and EVs market share on the planning decision, we consider different scenarios of EVs' driving range under increasing EVs' penetration. All EVs in the network are assumed to have relatively short ranges ($D^e \sim Gamma(30, 1.5)$, $\mathbb{E}[D^e] = 45$), medium ranges ($D^e \sim Gamma(50, 1.5)$, $\mathbb{E}[D^e] = 75$) or long ranges ($D^e \sim Gamma(70, 1.5)$, $\mathbb{E}[D^e] = 105$), respectively. Because charging infrastructure would probably not be erased and newly built for a gradual increase in demand, the charging station will be continuously used in later stages once it is deployed.

The summary of the optimal number of charging stations (NumS), the number of chargers (NumC) and associated costs, i.e. capital cost (CapCost) and expected system cost (SysCost) has been presented as in Table 3. The average run-time for each EVs' penetration level is 2.35 hours. The details on planning decision, associated times such as travel time and waiting time in each scenario and run-time for each EVs' proportion level can be seen in C.6, Appendix C. In general, the expected system cost tends to decrease when EVs' driving range increases while rising sharply when there are more EVs in the network. Besides, the investment cost accounts for a major proportion of expected system cost (59% - 97%), especially in the case of short driving range, which emphasizes the long-term impact of charging facilities planning. It can be seen that the capital cost, which results from the planning decision, is highly dependent on the traffic pattern on the network. Therefore, the inappropriate deployment of charging infrastructure can increase both congestion and investment cost, which is demonstrated in test-bed network 2.

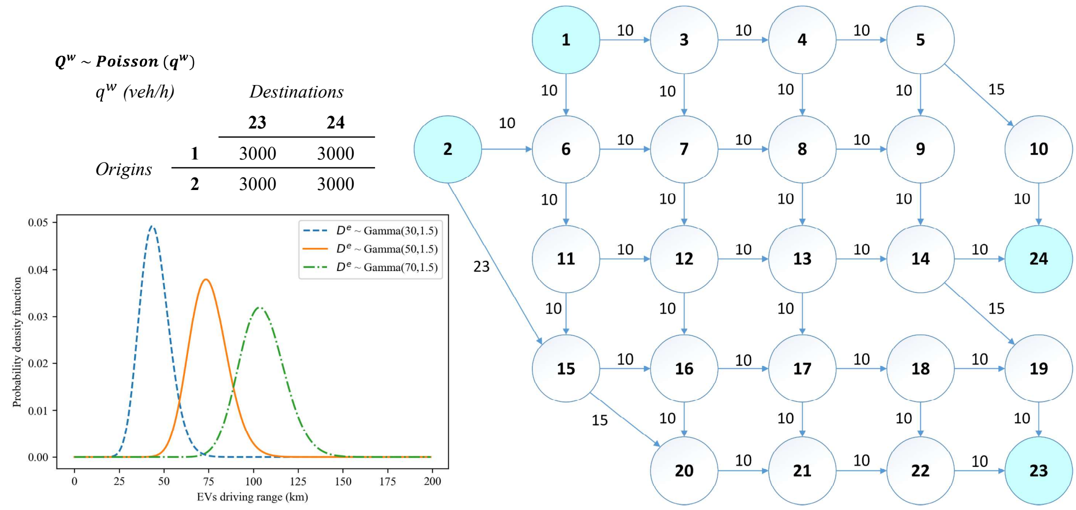

Figure 4: Test-bed network 1

Table 3: Investment and expected system cost for test-bed network 1

	$D^e \sim Gamma(30, 1.5)$ $\mathbb{E}[D^e] = 45$				$D^e \sim Gamma(50, 1.5)$ $\mathbb{E}[D^e] = 75$				$D^e \sim Gamma(70, 1.5)$ $\mathbb{E}[D^e] = 105$			
% EVs	NumS	NumC	**CapCost ($)**	**SysCost ($)**	NumS	NumC	**CapCost ($)**	**SysCost ($)**	NumS	NumC	**CapCost ($)**	**SysCost ($)**
10%	3	546	3,480,000	4,249,482	1	204	1,270,000	2,020,103	1	160	1,050,000	1,780,155
20%	3	1025	5,875,000	6,769,409	1	402	2,260,000	3,106,612	1	317	1,835,000	2,623,996
30%	3	1516	8,330,000	9,431,205	1	606	3,280,000	4,260,136	1	460	2,550,000	3,431,247
40%	3	2032	10,910,000	12,303,574	1	802	4,260,000	5,415,884	2	763	4,315,000	5,047,117
50%	5	2775	15,125,000	16,378,688	2	1153	6,265,000	7,278,328	2	874	4,870,000	5,590,707
60%	5	3135	16,925,000	18,408,536	3	1461	8,055,000	8,807,614	2	989	5,445,000	6,141,020
70%	6	3973	21,365,000	22,768,664	3	1595	8,725,000	9,429,029	2	1092	5,960,000	6,633,935
80%	7	4839	25,945,000	27,158,932	3	1736	9,430,000	10,076,058	2	1238	6,690,000	7,335,487
90%	8	5708	30,540,000	31,559,262	3	1885	10,175,000	10,827,161	2	1389	7,445,000	8,068,660
100%	8	6004	32,020,000	33,058,542	3	2037	10,935,000	11,504,731	2	1549	8,245,000	8,867,938

From an environmental perspective, using more EVs can reduce the total environmental cost caused by the pollutant emitted from GVs (Figure 5a). However, it can be seen from the heat map that in the case of short and medium driving range, the total environmental cost tends to increase slightly until EVs' penetration reaches 40%, then decreases significantly when there are more EVs. This phenomenon happens because of the on-route congestion in the network (Figure 7a). Because EVs' drivers with shorter driving range will have fewer options when choosing the route to reach their destination, it will cause more congestion and make GVs choose the longer paths. Therefore, the total environmental cost tends to be higher in the case of short driving range and reduces when the EVs' driving range increases.

Besides, Figure 6 illustrates the environmental cost under different scenarios of the EVs' driving range and the level of EVs' proportion. Following the same pattern of the total environmental cost, the shorter the EVs' driving range, the higher environmental cost per GV. The underlying reason is that when the EVs' driving range is short, EVs' users have to crowd through a limited number of paths. Therefore, it leads to more congestion on the network. When EVs' driving range is relatively long, the environmental cost per GV remains the same over the different levels of EVs' penetration on the network.

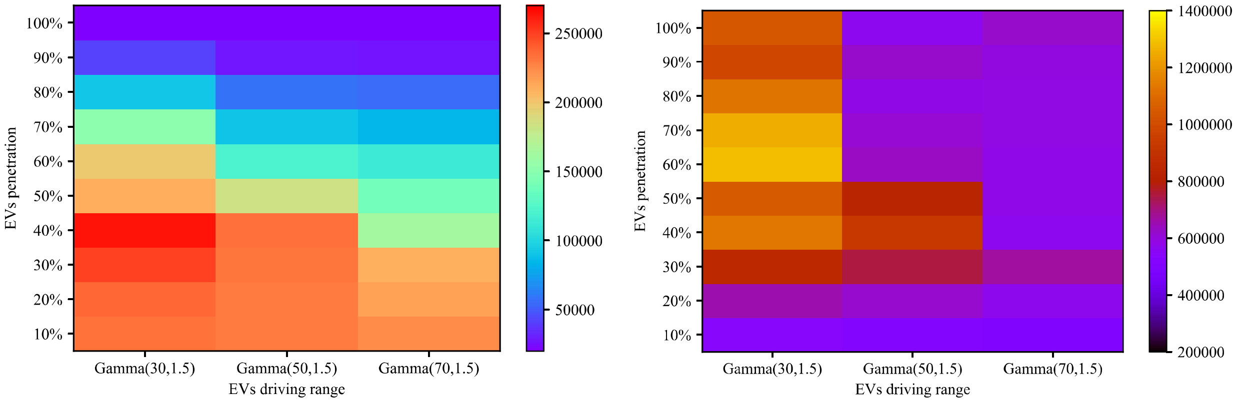

(a) (b)

Figure 5: (a) Heat-map of the expected environmental cost (\$). (b) Heat-map of the expected travel cost (\$).

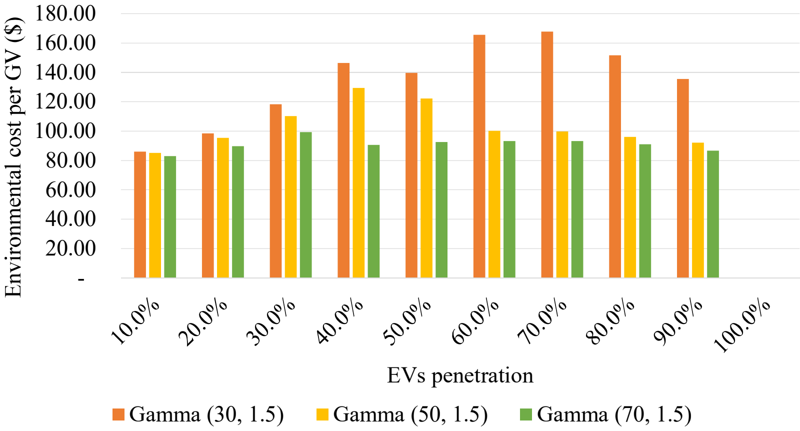

Figure 6: The environmental cost per GV

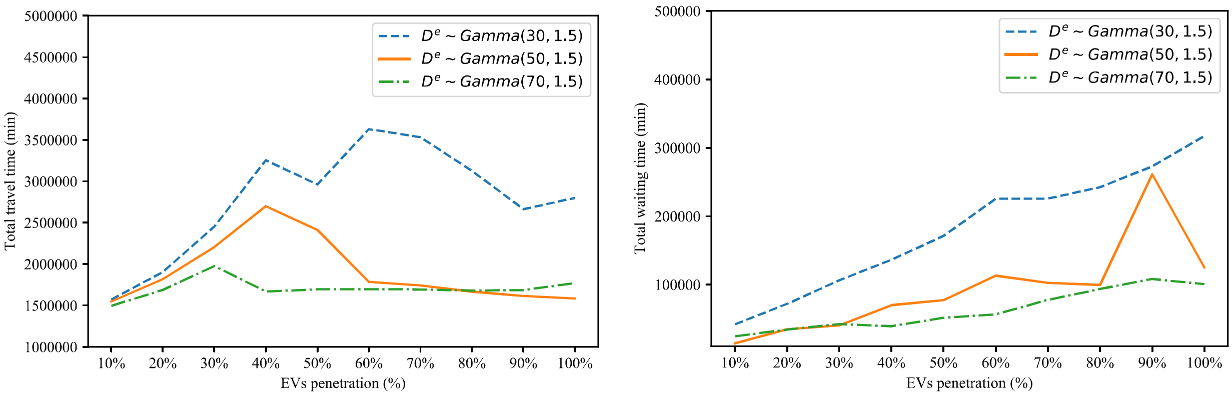

(a) (b)

Figure 7: (a) Total travel times. (b) Total waiting times.

As shown in Figures 7a and 7b, the charging congestion at the charging station contributes just a small amount compared to on-route congestion and can be reduced by increasing the driving range of EVs. The same conclusion can also be made by using Appendix C.

Meanwhile, the travel cost depends not only on the driving range and EVs proportion but also the number of charging facilities in the network (Figure 5b). On-route congestion tends to be more serious when EVs' penetration increases, but it can be reduced by improving the EVs' driving range and providing more charging facilities. Therefore, it is worth mentioning that both driving ranges, the EVs penetration and the number of charging facilities have a significant impact on the system performance.

A comparative analysis among different distributions has been conducted to investigate the impact of EVs' driving range distributions on the network performance with charging infrastructure. As the driving range must only take non-negative values, besides Gamma distribution, Weibull and Log-normal distributions can also be adopted (Miwa et al., 2017). The parameters of Weibull and Log-normal distributions have been chosen in the manner that the expected driving range of EVs is approximately 75 km. Therefore, we consider three scenarios of EVs driving range distributions: $D^e \sim Gamma(a = 50, b = 1.5)$, $D^e \sim Weibull(\alpha = 8, \beta = 80)$, and $D^e \sim Lognormal(\mu = 4.3, \sigma = 0.18)$.

The summary of total travel times (TTT), total waiting time (TWT), and environmental cost (EnvCost) under different scenarios have been shown in Table 4. Besides, the total waiting time under different distributions can be seen in Figure 8.

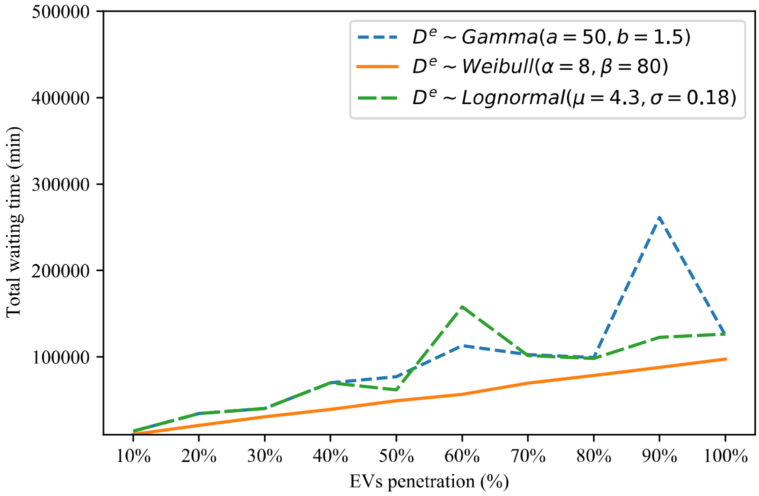

Figure 8: Total waiting time under different EVs' driving range distributions

Table 4: Network performance under different EVs' driving range distributions

	$D^e \sim Gamma(a = 50, b = 1.5)$ $\mathbb{E}[D^e] = 75$			$D^e \sim Weibull(\alpha = 8, \beta = 80)$ $\mathbb{E}[D^e] = 75$			$D^e \sim Lognormal(\mu = 4.3, \sigma = 0.18)$ $\mathbb{E}[D^e] = 75$		
% EVs	**TTT** (min)	**TWT** (min)	**EnvCost** ($)	**TTT** (min)	**TWT** (min)	**EnvCost** ($)	**TTT** (min)	**TWT** (min)	**EnvCost** ($)
10%	1,547,051	14,084	229,725	1,503,818	10,576	225,073	1,541,089	14,084	228,967
20%	1,817,526	34,582	229,243	1,692,847	20,849	218,349	1,822,746	34,582	229,452
30%	2,205,067	40,372	231,656	1,918,221	30,641	210,132	2,203,319	40,372	231,233
40%	2,698,946	69,960	232,916	2,171,349	39,379	199,943	2,686,645	69,960	231,942
50%	2,412,920	77,083	183,326	1,786,326	49,269	148,035	2,432,735	61,976	184,631
60%	1,783,925	113,015	120,300	1,786,496	56,675	121,086	1,800,942	158,091	121,768

continued . . .

. . . continued

	$D^e \sim Gamma(30, 1.5)$ $\mathbb{E}[D^e] = 45$			$D^e \sim Gamma(50, 1.5)$ $\mathbb{E}[D^e] = 75$			$D^e \sim Gamma(70, 1.5)$ $\mathbb{E}[D^e] = 105$		
% EVs	**TTT** (min)	**TWT** (min)	**EnvCost** ($)	**TTT** (min)	**TWT** (min)	**EnvCost** ($)	**TTT** (min)	**TWT** (min)	**EnvCost** ($)
70%	1,740,276	102,516	89,765	1,728,029	69,736	89,410	1,731,413	101,546	89,056
80%	1,666,142	99,365	57,556	1,655,771	78,600	57,461	1,672,554	98,366	58,068
90%	1,612,312	261,230	27,647	1,598,487	87,825	27,647	1,615,998	122,836	27,859
100%	1,584,124	125,068	-	1,560,371	97,332	-	1,577,136	126,275	-

Although the system performance is significantly affected by the expected driving range of EVs, it is insensitive to the shape of driving range distributions. Under the same expected driving range and charging infrastructure, the network's total travel time and environmental cost remain almost the same with different driving range distributions. However, the shape of driving range distributions greatly impacts the waiting time at charging stations. In reality, the distribution of EVs can be fitted from the survey data.

4.2. Test-bed network 2: A comparative study

In this subsection, we employ the proposed framework on a larger size network with 42 nodes and 80 links, as shown in Figure 9. In this case, the aggregate travel demands between each O-D pair are assumed to be Poisson with a mean (and variance) of 3,000 (veh/hr). Various EVs' penetrations are considered in which all EVs are assumed to follow Gamma distribution with the shape of 50 (km) and a scale of 1.5. Then we compare the results with those provided by the traditional two-stage optimization approach.

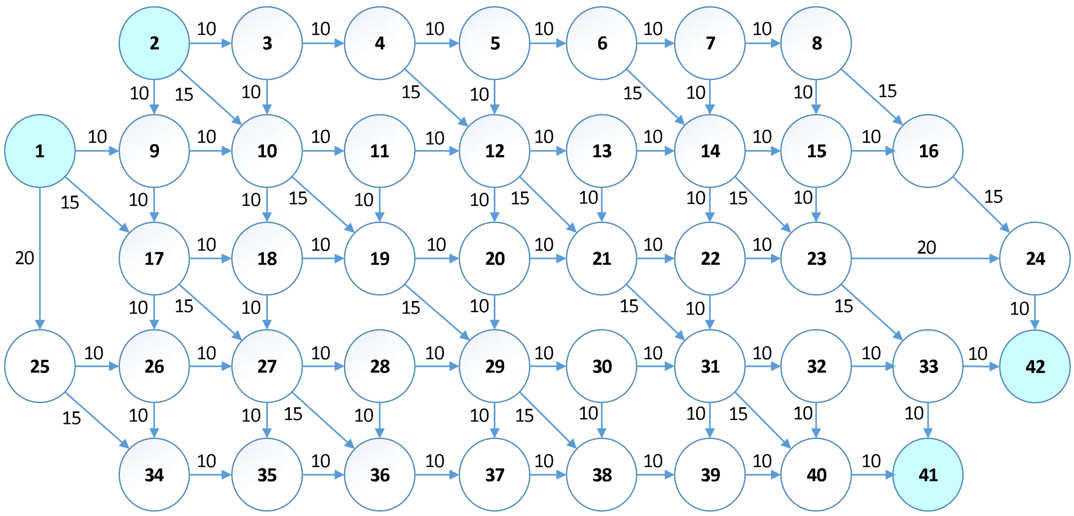

Figure 9: Test-bed network 2

In the two-stage approach, the travel demands are assumed to be not recognized in the first stage. Therefore, in this stage, the planner will try to optimize the locations of charging stations by ensuring every O-D pair will be covered. In other words, the first stage is to minimize the number of charging stations while ensuring at least one feasible path between each O-D pair. In the second stage, when the travel demands are fully recognized, the capacity of the charging station will be optimized in order to minimize the charging congestion. Because the two-stage approach is unable to capture the interaction between the planning decision and traffic pattern in the network, we also relax the constraint on continuous use of installed charging facilities in the CEM-based approach.

In the benchmark approach, the problem is solved by assuming that we firstly have limited information in hand and the flow pattern remains unchanged. Therefore, although it can provide a good solution when EVs' penetration is low, this approach witnesses the deterioration in network performance in the long-run, as shown in Figure 10. It can be seen from the numerical results that the CEM-based approach can yield better solutions in terms of congestion, capital cost and expected system cost due to its capability to describe the changing of travellers route choice behaviours. The final results are summarized in Table 5.

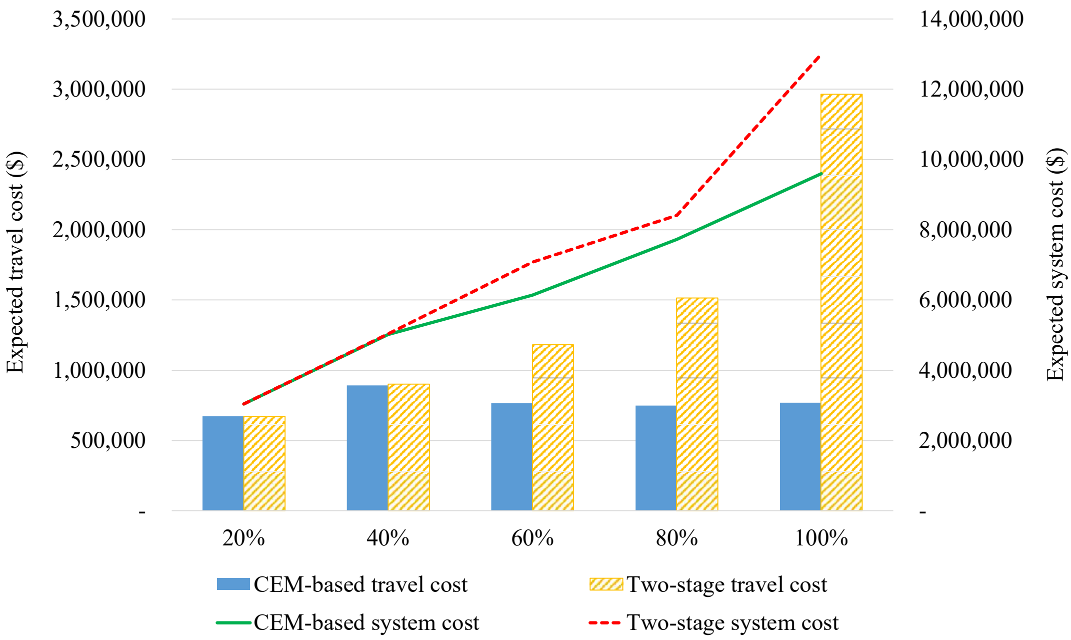

Figure 10: Comparison on expected travel costs and system costs between two approaches

Table 5: Final results for test-bed network 2

CEM-based approach					
% EVs	Planning decision	Expected environmental cost ($)	Expected travel cost ($)	Capital cost ($)	Expected system cost ($)
20%	$u_{21} = 371$	260,088.78	672,983.64	2,105,000.00	3,038,072.42
40%	$u_{21} = 726$	238,995.62	892,287.94	3,880,000.00	5,011,283.56
60%	$u_{14} = 317$ $u_{29} = 628$	146,430.79	767,188.33	5,225,000.00	6,138,619.12
80%	$u_{14} = 504$ $u_{29} = 777$	70,645.60	749,606.69	6,905,000.00	7,725,252.29
100%	$u_{14} = 718$ $u_{29} = 948$	-	769,033.78	8,830,000.00	9,599,033.78
Two-stage approach					
% EVs	Planning decision	Expected environmental cost ($)	Expected travel cost ($)	Capital cost ($)	Expected system cost ($)
20%	$u_{21} = 372$	259,667.66	671,070.17	2,110,000.00	3,040,737.83

continued ...

. . . continued

% EVs	Planning decision	Expected environmental cost ($)	Expected travel cost ($)	Capital cost ($)	Expected system cost ($)
40%	$u_{21} = 729$	241,949.92	900,028.99	3,895,000.00	5,036,978.92
60%	$u_{21} = 1090$	196,349.94	1,181,016.13	5,700,000.00	7,077,366.07
80%	$u_{21} = 1306$	110,741.13	1,513,834.41	6,780,000.00	8,404,575.54
100%	$u_{21} = 1630$	-	2,963,138.59	10,035,000.00	12,998,138.59

5. Concluding remarks

In this paper, we proposed a systematic framework to deploy the fast-charging facilities under stochastic driving range, uncertain demand and charging congestion as one of the first attempts to solve the charging location problem considering the highly stochastic nature of the problem. The problem has been solved to minimize the capital cost, network congestion (i.e., en-route and charging congestion) and environmental cost while capturing travellers' stochastic route choice behaviour using a bi-level optimization structure. Numerical tests have shown that the proposed CEM-based approach is able to provide a good solution for such a complex combinatorial optimization problem. Due to the ability to capture the mutual interaction between planning decision and traffic pattern, the present approach can avoid the deterioration in the network performance and yield a better solution compared to the two-stage approach.

However, the computational cost remains a burden, especially for large-scale networks. The bi-level optimization framework is a non-linear and non-convex optimization problem in which there is no single approach to obtain a general global optimal solution. To better understand the resulting quality of the problem and reduce the computational cost, the bi-level program might be reformulated as a mathematical program with equilibrium constraints (MPEC). Due to the complexity of the multi-class probit-based SUE traffic assignment problem with stochastic demand, we leave this problem for future study, which is part of the authors' on-going research. Moreover, in order to capture the range anxiety, the proposed model could be extended to track the SOC through a journey as a function of travel time or travel distance. Then a profile of SOC and the range anxiety can be adopted to compute the expected accumulated range anxiety through charging stations to the end of the trip, assuming a random distance that travellers can complete between charging stations.

Appendix A. Cross-entropy Method

Given that the location of charging stations and number of chargers are independent random variables with the $(|K| \times m)$ success probabilities matrix γ, where $|K|$ is the number of nodes in the network and m is the maximum number of chargers that can be located at one station. The vector of feasible paths $(\mathbf{y})$ corresponding to the charging locations can be identified by the deterministic equivalence of chance constraints on driving range.

$$\gamma = \begin{pmatrix} \gamma_{1,0} & \gamma_{1,1} & \cdots & \gamma_{1,m} \\ \gamma_{2,0} & \gamma_{2,2} & \cdots & \gamma_{2,m} \\ \vdots & \vdots & \ddots & \vdots \\ \gamma_{|K|,0} & \gamma_{|K|,2} & \cdots & \gamma_{|K|,m} \end{pmatrix} \tag{A.1}$$

Accordingly, our problem is to minimize the cost function PI($\mathbf{X}$, $\mathbf{f(X)}$) over all $\mathbf{X(x,\ u,\ y)}$ in set Ω:

$$z^* = \min_{\mathbf{X}\in\Omega} PI(\mathbf{X}, \mathbf{f}(\mathbf{X})) \tag{A.2}$$

The above optimization problem can be associated with an estimation problem $l(z) = \mathbb{P}(PI(\mathbf{X_n}, \mathbf{f}(\mathbf{X_n})) \leq z)$, where $\mathbf{X_n}$ is chosen on Ω from a probability density function $f(\mathbf{X}, \gamma)$ with sample size N and z is close to (but greater than) z^*. Generally, $l(z)$ is a rare-event probability. As presented in De Boer et al. (2005), CEM approach can be used to find an importance sampling distribution so that all its mass concentrates in a neighborhood of $\mathbf{X}^*$. Therefore, the optimal or near optimal states can be obtained by sampling from such a distribution.

To describe parameterized random mechanism for generating the charging solutions, we consider a solution $X = (X_1, ..., X_{|K|})$ has $|K|$ independent components such that $X_i = j$ with probability $\gamma_{i,j}$, $i = 1, ..., |K|; j = 1, ..., m$. Then, the parameter of sampling distribution at the t^{th} iteration can be updated using following formula (Botev et al., 2013).

$$\hat{\gamma}_{i,j}^{(t)} = \frac{\sum_{k=1}^{N} I_{\{(PI(\mathbf{X_k}, \mathbf{f}(\mathbf{X_k})) \leq z)\}} I_{\{X_{k,i}=j\}}}{\sum_{k=1}^{N} I_{\{(PI(\mathbf{X_k}, \mathbf{f}(\mathbf{X_k})) \leq z)\}}}, \qquad i = 1, ..., |K|; j = 1, ..., m \tag{A.3}$$

With the charging solution $\mathbf{X}$, the vector of equilibrium path flow $\mathbf{f(X)}$ can be obtained by solving the multi-class probit-based SUE model with Poisson demand. As mentioned above, the multi-class probit-based SUE model based on the Poisson-corrected travel time function is adopted to identify route choice probabilities. The link perception errors are assumed to be the same for all vehicle classes and independently distributed for link a as normal distribution, $Nor(0, (\phi t_a(0))^2)$, with $\phi = 0.3$ used in numerical tests (Clark and Watling, 2005). The SUE is estimated using the route-based Method of Successive Average (MSA) as summarized in Algorithm 2.

Appendix B. Arrival rates determination

Furthermore, to project the waiting time at charging stations, we first need to identify the arrival rates of EVs to the stations. Let l is the maximum length that $\mathbb{P}(D^n \leq l)$ is smaller than risk level α. Considering a path consisting of node sequence with three charging stations (at node 2, node 3 and node 4) and link lengths (km) as in Figure B.11.

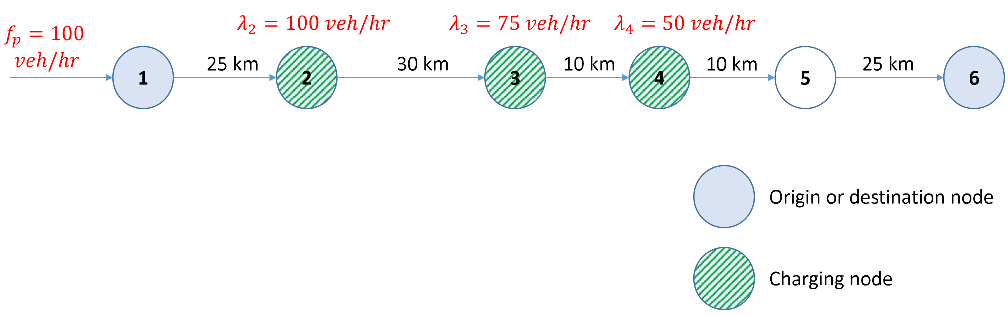

Figure B.11: An illustration of arrival rates calculation

Assuming that EVs flow on this path is $f_p = 100$ veh/hr with $l = 50$ km, it is clear that EVs' travellers only reach the destination (node 6) when they recharge at node 3 or node 4. Therefore, it is reasonable to assume that the same proportions of travellers decided to recharge either at node 3 or node 4. Next, to reach the charging station at node 4, travellers can recharge either at node 2 or node 3. Using the same reason mechanism, we can calculate all arrival rates at charging stations on a path using corresponding EVs path flows. Finally, the aggregate arrival rates would be the sum of arrival rates on paths.

Appendix C. Test-bed network 1: Planning decision, travel time and waiting time

Table C.6: Planning decision, travel time and waiting time for test-bed network 1

	$D^e \sim Gamma(30, 1.5)$ $\mathbb{E}[D^e] = 45$				$D^e \sim Gamma(50, 1.5)$ $\mathbb{E}[D^e] = 75$				$D^e \sim Gamma(70, 1.5)$ $\mathbb{E}[D^e] = 105$			
% EVs	Planning decision	**Travel time** (hr)	**Waiting time** (hr)	**Run-time** (hr)	Planning decision	**Travel time** (hr)	**Waiting time** (hr)	**Run-time** (hr)	Planning decision	**Travel time** (hr)	**Waiting time** (hr)	**Run-time** (hr)
10%	$u_7 = 201$ $u_{13} = 207$ $u_{21} = 138$	26,177	698	1.42	$u_{13} = 204$	25,784	235	2.84	$u_{11} = 160$	24,911	406	1.35
20%	$u_7 = 414$ $u_{13} = 402$ $u_{21} = 209$	31,721	1,196	2.26	$u_{13} = 402$	30,292	576	3.39	$u_{11} = 317$	28,119	569	0.95
30%	$u_7 = 603$ $u_{13} = 606$ $u_{21} = 307$	40,865	1,769	2.12	$u_{13} = 606$	36,751	673	3.15	$u_{11} = 460$	32,930	704	0.78
40%	$u_7 = 803$ $u_{13} = 819$ $u_{21} = 410$	54,230	2,270	1.80	$u_{13} = 802$	44,982	1,166	2.78	$u_{11} = 464$ $u_{16} = 299$	27,802	651	0.54
50%	$u_7 = 815$ $u_{13} = 820$ $u_{15} = 230$ $u_{16} = 381$ $u_{21} = 529$	49,352	2,853	2.22	$u_{13} = 806$ $u_{16} = 347$	40,215	1,285	2.77	$u_{11} = 476$ $u_{16} = 398$	28,234	858	0.57
60%	$u_7 = 914$ $u_{13} = 827$ $u_{15} = 291$ $u_{16} = 473$ $u_{21} = 630$	60,487	3,756	1.99	$u_4 = 264$ $u_{13} = 810$ $u_{16} = 387$	29,732	1,884	2.48	$u_{11} = 480$ $u_{16} = 509$	28,267	942	0.52
70%	$u_7 = 1072$ $u_9 = 910$ $u_{13} = 378$ $u_{15} = 502$ $u_{16} = 408$ $u_{21} = 703$	58,874	3,761	2.20	$u_4 = 318$ $u_{13} = 811$ $u_{16} = 466$	29,005	1,709	2.36	$u_{11} = 488$ $u_{16} = 604$	28,212	1,293	0.62

continued ...

... continued

	$D^e \sim Gamma(30, 1.5)$ $\mathbb{E}[D^e] = 45$				$D^e \sim Gamma(50, 1.5)$ $\mathbb{E}[D^e] = 75$				$D^e \sim Gamma(70, 1.5)$ $\mathbb{E}[D^e] = 105$			
% EVs	**Planning decision**	**Travel time** (hr)	**Waiting time** (hr)	**Run-time** (hr)	Planning decision	**Travel time** (hr)	**Waiting time** (hr)	**Run-time** (hr)	Planning decision	**Travel time** (hr)	**Waiting time** (hr)	**Run-time** (hr)
80%	$u_7 = 1249$ $u_9 = 409$ $u_{13} = 994$ $u_{15} = 398$ $u_{16} = 643$ $u_{18} = 443$ $u_{21} = 703$	52,108	4,037	1.83	$u_4 = 362$ $u_{13} = 818$ $u_{16} = 556$	27,769	1,656	2.89	$u_{11} = 527$ $u_{16} = 711$	27,983	1,559	0.65
90%	$u_7 = 1258$ $u_9 = 449$ $u_{11} = 504$ $u_{13} = 1000$ $u_{15} = 447$ $u_{16} = 827$ $u_{18} = 488$ $u_{21} = 735$	44,385	4,546	1.68	$u_4 = 401$ $u_{13} = 843$ $u_{16} = 641$	26,872	4,354	2.79	$u_{11} = 583$ $u_{16} = 806$	28,080	1,803	0.67
100%	$u_7 = 1281$ $u_9 = 541$ $u_{11} = 521$ $u_{13} = 1047$ $u_{15} = 460$ $u_{16} = 835$ $u_{18} = 528$ $u_{21} = 791$	46,642	5,285	0.93	$u_4 = 469$ $u_{13} = 846$ $u_{16} = 722$	26,402	2,084	1.32	$u_{11} = 644$ $u_{16} = 905$	29,472	1,675	0.56

Appendix D. Test-bed network 3: Bi-directional network

Consider a medium-sized network with 24 nodes and 42 links as in Figure D.12a. The travel demand and network parameters have been adopted from Numerical tests. In this test, the EVs are assumed to account 50% of total travel demand and have medium driving ranges ($D^e \sim Gamma(a = 50, b = 1.5)$). The charging planning decisions under this scenario is shown in Figure D.12b.

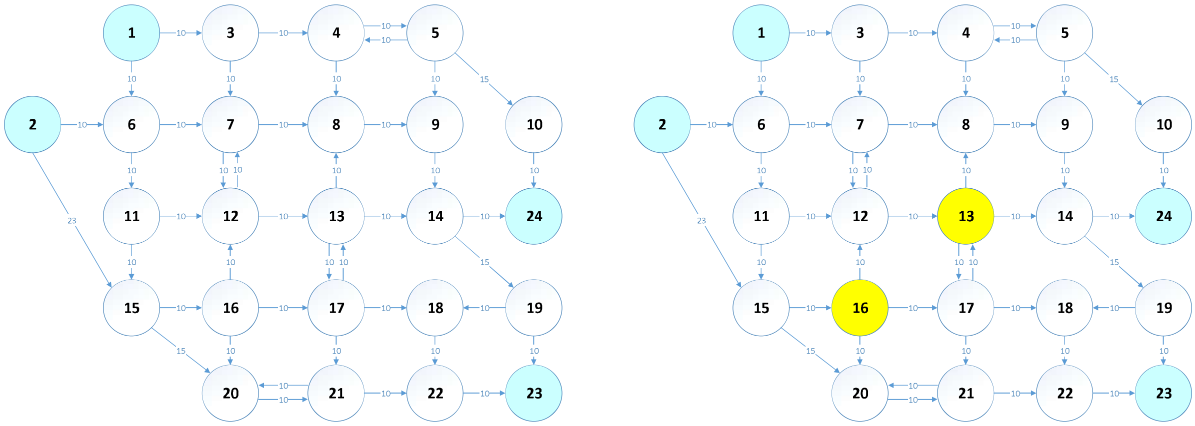

(a) Initial network (b) Charging location decisions (50% EVs)

Figure D.12: Test-bed network 3

Table D.7 depicts the optimal number of stations (NumS), number of chargers (NumC), and network performances, i.e., the capital cost, travel time, waiting time, travel cost, environmental cost, and system cost.

Table D.7: Final results for test-bed network 3 (50% EVs)

NumS	**NumC**	**Capital Cost** (\$)	**Travel time** (min)	**Waiting time** (min)	**Travel cost** (\$)	**Environmental cost** (\$)	**System cost** (\$)
2	1,020	5,630,000	3,019,914	62,200	1,027,371	211,433	6,868,804

The convergence of PI solutions and standard deviation of best PI values over iterations has been illustrated in Figure D.13a and Figure D.13b. The computational time is 5.03 hours.

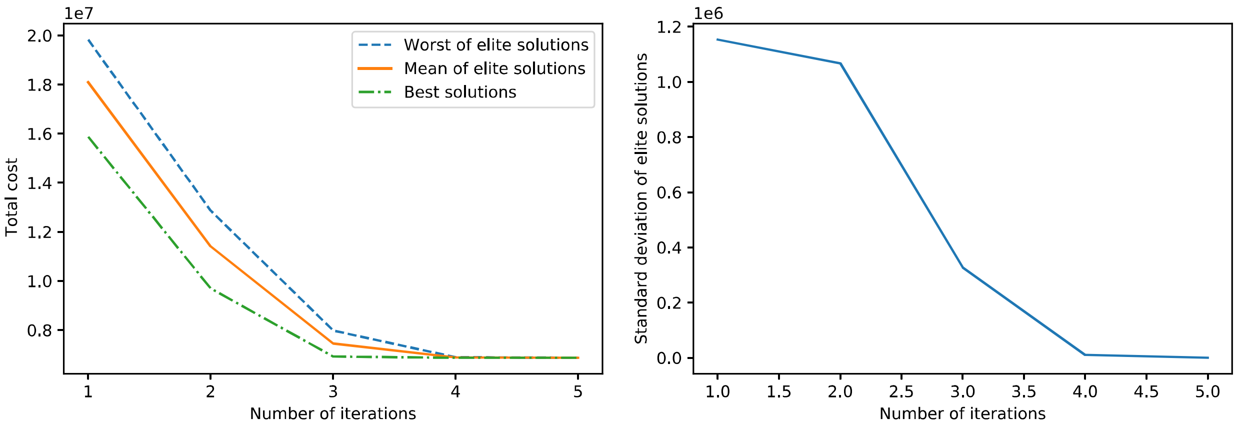

(a) (b)

Figure D.13: Convergence of PI values over iterations

References

Abudayyeh, D., Ngoduy, D., Nicholson, A., 2018. Traffic signal optimisation in disrupted networks with re-routing. Transportation Research Procedia 34, 195–202.

Abudayyeh, D., Nicholson, A., Ngoduy, D., 2021. Traffic signal optimisation in disrupted networks, to improve resilience and sustainability. Travel Behaviour and Society 22, 117–128.

Berman, O., Drezner, Z., 2007. The multiple server location problem. Journal of the Operational Research Society 58, 91–99.

Botev, Z.I., Kroese, D.P., Rubinstein, R.Y., L'Ecuyer, P., 2013. The cross-entropy method for optimization, in: Handbook of statistics. Elsevier. volume 31, pp. 35–59.

Boujelben, M.K., Gicquel, C., 2019. Efficient solution approaches for locating electric vehicle fast charging stations under driving range uncertainty. Computers & Operations Research 109, 288–299.

Church, R.L., Meadows, M.E., 1979. Location modeling utilizing maximum service distance criteria. Geographical Analysis 11, 358–373.

Clark, S., Watling, D., 2005. Modelling network travel time reliability under stochastic demand. Transportation Research Part B: Methodological 39, 119–140.

De Boer, P.T., Kroese, D.P., Mannor, S., Rubinstein, R.Y., 2005. A tutorial on the cross-entropy method. Annals of operations research 134, 19–67.

Dong, J., Lin, Z., 2014. Stochastic modeling of battery electric vehicle driver behavior: impact of charging infrastructure deployment on the feasibility of battery electric vehicles. Transportation Research Record 2454, 61–67.

Earl, T., Mathieu, L., Cornelis, S., Kenny, S., Ambel, C.C., Nix, J., 2018. Analysis of long haul battery electric trucks in eu, in: Commercial Vehicle Workshop, Graz.

EVSE, 2019. How much does it cost to set up an ev charging station? URL: https://evse.com.au/blog/evchargercost/.

Ghamami, M., 2019. Electric Vehicle Charger Placement Optimization in Michigan: Phase I-Highways. Technical Report. Technical Report.

Guo, F., Yang, J., Lu, J., 2018. The battery charging station location problem: Impact of users' range anxiety and distance convenience. Transportation Research Part E: Logistics and Transportation Review 114, 1–18.

He, F., Yin, Y., Lawphongpanich, S., 2014. Network equilibrium models with battery electric vehicles. Transportation Research Part B: Methodological 67, 306–319.

He, J., Yang, H., Tang, T.Q., Huang, H.J., 2018. An optimal charging station location model with the consideration of electric vehicle's driving range. Transportation Research Part C: Emerging Technologies 86, 641–654.

He, S.Y., Kuo, Y.H., Wu, D., 2016. Incorporating institutional and spatial factors in the selection of the optimal locations of public electric vehicle charging facilities: A case study of beijing, china. Transportation Research Part C: Emerging Technologies 67, 131–148.

Hodgson, M.J., 1990. A flow-capturing location-allocation model. Geographical Analysis 22, 270–279.

Hosseini, M., MirHassani, S., 2015. Refueling-station location problem under uncertainty. Transportation Research Part E: Logistics and Transportation Review 84, 101–116.

Hosseini, M., MirHassani, S., Hooshmand, F., 2017. Deviation-flow refueling location problem with capacitated facilities: Model and algorithm. Transportation Research Part D: Transport and Environment 54, 269–281.

Huang, Y., Kockelman, K.M., 2020. Electric vehicle charging station locations: Elastic demand, station congestion, and network equilibrium. Transportation Research Part D: Transport and Environment 78, 102179.

Huber, J., Dann, D., Weinhardt, C., 2020. Probabilistic forecasts of time and energy flexibility in battery electric vehicle charging. Applied Energy 262, 114525.

IEA, 2019. Global ev outlook 2019. URL: www.iea.org/publications/reports/globalevoutlook2019/.

Jiang, N., Xie, C., Duthie, J.C., Waller, S.T., 2014. A network equilibrium analysis on destination, route and parking choices with mixed gasoline and electric vehicular flows. EURO Journal on Transportation and Logistics 3, 55–92.

Jing, W., An, K., Ramezani, M., Kim, I., 2017. Location design of electric vehicle charging facilities: A path-distance constrained stochastic user equilibrium approach. Journal of Advanced Transportation 2017.

Jung, J., Chow, J.Y., Jayakrishnan, R., Park, J.Y., 2014. Stochastic dynamic itinerary interception refueling location problem with queue delay for electric taxi charging stations. Transportation Research Part C: Emerging Technologies 40, 123–142.

Kim, J.G., Kuby, M., 2012. The deviation-flow refueling location model for optimizing a network of refueling stations. International Journal of Hydrogen Energy 37, 5406–5420.

Kuby, M., Lim, S., 2005. The flow-refueling location problem for alternative-fuel vehicles. Socio-Economic Planning Sciences 39, 125–145.

Lee, C., Han, J., 2017. Benders-and-price approach for electric vehicle charging station location problem under probabilistic travel range. Transportation Research Part B: Methodological 106, 130–152.

Lee, Y.G., Kim, H.S., Kho, S.Y., Lee, C., 2014. User equilibrium–based location model of rapid charging stations for electric vehicles with batteries that have different states of charge. Transportation research record 2454, 97–106.

Li, S., Huang, Y., 2014. Heuristic approaches for the flow-based set covering problem with deviation paths. Transportation Research Part E: Logistics and Transportation Review 72, 144–158.

Maher, M., Liu, R., Ngoduy, D., 2013. Signal optimisation using the cross entropy method. Transportation Research Part C: Emerging Technologies 27, 76–88.

Miwa, T., Sato, H., Morikawa, T., 2017. Range and battery depletion concerns with electric vehicles. Journal of Advanced Transportation 2017.

Nakayama, S., Watling, D., 2014. Consistent formulation of network equilibrium with stochastic flows. Transportation Research Part B: Methodological 66, 50–69.

Ngo, H., Kumar, A., Mishra, S., 2020. Optimal positioning of dynamic wireless charging infrastructure in a road network for battery electric vehicles. Transportation Research Part D: Transport and Environment 85, 102385.

Ngoduy, D., Maher, M., 2012. Calibration of second order traffic models using continuous cross entropy method. Transportation Research Part C: Emerging Technologies 24, 102–121.

Nozick, L., 2001. The fixed charge facility location problem with coverage restrictions. Transportation Research Part E: Logistics and Transportation Review 37, 281–296.

Ozbay, K., Bartin, B., Berechman, J., 2001. Estimation and evaluation of full marginal costs of highway transportation in new jersey. Journal of Transportation and Statistics 4, 81–103.

Penic, M.A., Upchurch, J., 1992. Transyt-7f: enhancement for fuel consumption, pollution emissions, and user costs. Transportation Research Record .

Rubinstein, R.Y., Kroese, D.P., 2004. The cross-entropy method: a unified approach to combinatorial optimization, Monte-Carlo simulation and machine learning. Springer Science & Business Media.

Sheffi, Y., 1985. Urban transportation networks. volume 6. Prentice-Hall, Englewood Cliffs, NJ.

Shen, Z.J.M., Feng, B., Mao, C., Ran, L., 2019. Optimization models for electric vehicle service operations: A literature review. Transportation Research Part B: Methodological .

Tran, C.Q., Ngoduy, D., Keyvan-Ekbatani, M., Watling, D., 2021. A user equilibrium-based fast-charging location model considering heterogeneous vehicles in urban networks. Transportmetrica A: Transport Science 17, 439–461.

Upchurch, C., Kuby, M., Lim, S., 2009. A model for location of capacitated alternative-fuel stations. Geographical Analysis 41, 85–106.

Varga, B.O., Sagoian, A., Mariasiu, F., 2019. Prediction of electric vehicle range: A comprehensive review of current issues and challenges. Energies 12, 946.

de Vries, H., Duijzer, E., 2017. Incorporating driving range variability in network design for refueling facilities. Omega 69, 102–114.

Wang, Y.W., Lin, C.C., 2009. Locating road-vehicle refueling stations. Transportation Research Part E: Logistics and Transportation Review 45, 821–829.

Wu, F., Sioshansi, R., 2017. A stochastic flow-capturing model to optimize the location of fast-charging stations with uncertain electric vehicle flows. Transportation Research Part D: Transport and Environment 53, 354–376.

Xiao, D., An, S., Cai, H., Wang, J., Cai, H., 2020. An optimization model for electric vehicle charging infrastructure planning considering queuing behavior with finite queue length. Journal of Energy Storage 29, 101317.

Xie, C., Jiang, N., 2016. Relay requirement and traffic assignment of electric vehicles. Computer-Aided Civil and Infrastructure Engineering 31, 580–598.

Xie, F., Liu, C., Li, S., Lin, Z., Huang, Y., 2018. Long-term strategic planning of inter-city fast charging infrastructure for battery electric vehicles. Transportation Research Part E: Logistics and Transportation Review 109, 261–276.

Xu, M., Meng, Q., 2020. Optimal deployment of charging stations considering path deviation and nonlinear elastic demand. Transportation Research Part B: Methodological 135, 120–142.

Xu, M., Meng, Q., Liu, K., 2017. Network user equilibrium problems for the mixed battery electric vehicles and gasoline vehicles subject to battery swapping stations and road grade constraints. Transportation Research Part B: Methodological 99, 138–166.

Xu, M., Yang, H., Wang, S., 2020. Mitigate the range anxiety: Siting battery charging stations for electric vehicle drivers. Transportation Research Part C: Emerging Technologies 114, 164–188.

Yang, J., Guo, F., Zhang, M., 2017. Optimal planning of swapping/charging station network with customer satisfaction. Transportation Research Part E: Logistics and Transportation Review 103, 174–197.

Yıldız, B., Olcaytu, E., Şen, A., 2019. The urban recharging infrastructure design problem with stochastic demands and capacitated charging stations. Transportation Research Part B: Methodological 119, 22–44.

Yin, Y., Li, Z.C., Lam, W.H., Choi, K., 2014. Sustainable toll pricing and capacity investment in a congested road network: a goal programming approach. Journal of Transportation Engineering 140, 04014062.

Zhang, X., Rey, D., Waller, S.T., 2018. Multitype recharge facility location for electric vehicles. Computer-Aided Civil and Infrastructure Engineering 33, 943–965.

Zheng, H., He, X., Li, Y., Peeta, S., 2017. Traffic equilibrium and charging facility locations for electric vehicles. Networks and Spatial Economics 17, 435–457.

Zhong, R., Fu, K., Sumalee, A., Ngoduy, D., Lam, W., 2016. A cross-entropy method and probabilistic sensitivity analysis framework for calibrating microscopic traffic models. Transportation Research Part C: Emerging Technologies 63, 147–169.